

# Spectroscopy of higher harmonics in dynamic atomic force microscopy

Robert W Stark

Centre for Nanoscience and Section Crystallography, Ludwig-Maximilians-Universität,  
Theresienstraße 41, 80333 München, Germany

E-mail: stark@nanomanipulation.de

Received 19 September 2003

Published 22 December 2003

Online at [stacks.iop.org/Nano/15/347](http://stacks.iop.org/Nano/15/347) (DOI: 10.1088/0957-4484/15/3/020)

## Abstract

Dynamic atomic force microscopy (AFM) is a standard technique for imaging and the analysis of surfaces at the nanometre scale. In order to estimate material properties from the microscope data it is important to understand the nonlinear dynamics in the tip–sample interaction. Here, the system response of a tapping-mode atomic force microscope is investigated with numerical simulations. In the numerical model, the AFM cantilever is treated as a distributed parameter system that is capable of higher eigenmode excitation. With this multiple-degree-of-freedom (MDOF) approach the generation of higher harmonics as well as the generation of subharmonics is analysed. Under typical imaging conditions higher harmonics are generated whereas a closer approach to the specimen surface can lead to a complicated dynamics.

(Some figures in this article are in colour only in the electronic version)

 This article features online multimedia enhancements

## 1. Introduction

For surface analysis with nanometre resolution, atomic force microscopy (AFM) has become an indispensable tool. Dynamic AFM methods like tapping mode or non-contact mode are widely used for imaging although a theoretical understanding of the data can be difficult due to the nonlinear tip–sample interaction [1]. In the tapping or amplitude modulation mode of operation, the force sensing cantilever is resonantly forced to free oscillations of about 10–100 nm amplitude. The cantilever is brought close to the specimen, where the tip periodically interacts with the surface in a way that can be conceived of as a strongly nonlinear output feedback limiting the oscillation amplitude [2].

The dynamics of tapping-mode AFM has been investigated using a single-degree-of-freedom (SDOF) approximation by several authors. It was shown that the nonlinear interaction can give rise to a complex dynamics although the system is well behaved for a large set of parameters [3–5]. A periodic orbit of the tip motion exists for a wide range of typical imaging conditions [6]. The possibility of chaotic motion was shown using the Melnikov method [7, 8]. Additionally, the existence of double [9] and higher period orbits [4] under

different operating conditions were investigated theoretically and experimentally [10]. The nonlinearity of the tip–sample contact also leads to the generation of higher harmonics in the system response. Thus, the interaction force is encoded in the harmonics of the system response. The occurrence of higher harmonic signals has been analysed theoretically employing multiple-degree-of-freedom (MDOF) models [2, 11–14].

Experimentally, the transient tip–sample interaction forces can be obtained by an inversion of the signal formation process [15], which requires a full spectral analysis. In a simplified approach, the tip–surface interaction can be investigated by means of dynamic force distance spectroscopy of higher harmonic signals [16]. It was shown that the harmonics can be used as a straightforward measure in order to investigate the tip–sample interaction.

To understand tip–sample forces during imaging as well as during nanomanipulation, the analysis of the entire spectral response can provide valuable insights. In the following, the response of the higher harmonics in dynamic AFM spectroscopy will be investigated by numerical simulations. To account for the nature of the microcantilever as a distributed parameter system, a state-space approach is used where multiple degrees of freedom are included in the simulation.

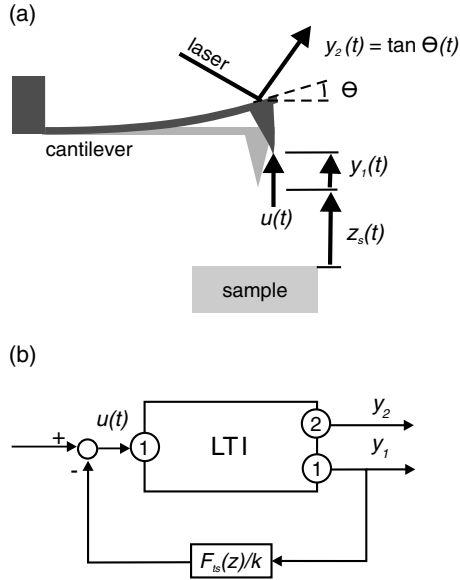


**Figure 1.** (a) Schematic of an atomic force microscope and (b) its representation by a linear system with a nonlinear output feedback. The force  $u(t)$  acting on the tip is fed into the linear time invariant system. The tip position  $y_1$  and the light lever readout  $y_2$  are the system outputs.

## 2. Modelling

The flexible cantilever in AFM is considered a linear and time invariant (LTI) system because in typical operating conditions its deflection is of the order of a few nanometres, whereas its thickness is in the range of microns. Thus, the physical system as sketched in figure 1(a) can be modelled as an LTI system with a nonlinear output feedback (figure 1(b)). To focus the following discussion on the basic phenomena, only forces that act on the tip, i.e. at input (1), will be considered. A magnetic or electrostatic excitation in the experiment corresponds to a driving force at input (1) in the model.

Considering  $n$  degrees-of-freedom (eigenmodes) of the cantilever, the state-space form of the equations of motion is given by

$$\dot{\mathbf{x}} = \mathbf{A}\mathbf{x} + \mathbf{b}u \quad (1)$$

$$\mathbf{y} = \mathbf{C}\mathbf{x} + \mathbf{d}u. \quad (2)$$

The time dependent state-vector  $\mathbf{x} = (x_1, \dot{x}_1, \dots, x_n, \dot{x}_n)$  consists of the displacements and velocities of the respective eigenmode. The system matrix

$$\mathbf{A} = \begin{bmatrix} \Phi_1 & 0 & 0 \\ 0 & \ddots & 0 \\ 0 & 0 & \Phi_n \end{bmatrix}, \quad \text{with } \Phi_i = \begin{bmatrix} 0 & 1 \\ -\hat{\omega}_i^2 & -2\gamma_i\hat{\omega}_i \end{bmatrix} \quad (3)$$

is a  $2n \times 2n$  matrix that contains the normalized eigenfrequencies  $\hat{\omega}_i = \omega_i/\omega_1$  and damping  $\gamma_i$  of each mode in  $2 \times 2$  submatrices  $\Phi_i$  along the diagonal. Thus, we assume that the cantilever is only weakly damped, as is the case in vacuum or ambient conditions. In the case of heavy damping, such as in a liquid environment, the matrix  $\mathbf{A}$  also contains non-diagonal elements, which leads to complex modes. The input vector

$$\mathbf{b} = [0, \varphi_1(\xi_{\text{tip}})/M_1, \dots, 0, \varphi_n(\xi_{\text{tip}})/M_n]^T \quad (4)$$

consists of the modal deflection of the cantilever at the tip  $\varphi_i(\xi_{\text{tip}})$  normalized by the generalized modal mass  $M_i = \int_0^1 m\varphi_i(\xi)^2 d\xi$ . Scalar  $u$  is the input to the model, i.e. the driving force minus the tip-sample interaction force.

The components of the output vector  $\mathbf{y} = [y_1, y_2]^T$ , i.e. the tip displacement output  $y_1$  that is used for feedback and the photo diode signal output  $y_2$ , are linear combinations of the states as defined in the output matrix

$$\mathbf{C} = \begin{bmatrix} \varphi_1(\xi_{\text{tip}})/n_{\text{pos}} & 0 & \cdots & \varphi_n(\xi_{\text{tip}})/n_{\text{pos}} & 0 \\ \varphi_1'(\xi_{\text{sens}})/n_{\text{sig}} & 0 & \cdots & \varphi_n'(\xi_{\text{sens}})/n_{\text{sig}} & 0 \end{bmatrix}. \quad (5)$$

The tip deflection output (1) is normalized with  $n_{\text{pos}}$  to obtain a unit dc gain, i.e. it is normalized to a spring constant  $\hat{k}_{\text{cant}} = 1$ . The optical lever sensor output (2) is normalized by  $n_{\text{sig}}$  to a unit response at  $\omega = 0$ . This follows the usual convention of calibrating the response of the light lever sensor. The direct transmission vector is zero

$$\mathbf{d} = \mathbf{0} \quad (6)$$

since there is no feed through from the force input (1) to the outputs (1) and (2) of the system.

From output (1) the tip displacement  $y_1 = \sum_{i=1}^n x_{2i-1}$  is fed back through the nonlinear tip-sample interaction force  $F_{\text{ts}}(y_1 + z_s)/k$  to input (1) of the model. The parameter  $z_s$  is the gap between the tip of the undeflected cantilever and the surface. Thus,  $y_1 + z_s$  is the distance between the actual tip position and the sample surface (figure 1(a)). Since the dc gain at output (1) of the LTI system is normalized to  $\hat{k}_{\text{cant}} = 1$ , the tip-sample forces have to be scaled with the spring constant  $k$ . The attractive part of the interaction force ( $y_1 + z_s \geq a_0$ ) is modelled as a van der Waals interaction force. In the case of negligible energy dissipation in the tip-sample contact, a Derjaguin-Müller-Toporov (DMT) model [17] can be used in the repulsive regime ( $y_1 + z_s < a_0$ ). Thus, the interaction force is

$$F_{\text{ts}}(y_1) = \begin{cases} -HR/[6(y_1 + z_s)^2] & y_1 + z_s \geq a_0, \\ -HR/6a_0^2 + \frac{4}{3}E^*\sqrt{R}(a_0 + y_1 + z_s)^{3/2} & y_1 + z_s < a_0 \end{cases} \quad (7)$$

where  $H$  is the Hamaker constant,  $R$  the tip radius and  $a_0$  an interatomic distance. The effective contact stiffness is given by  $E^* = [(1 - \nu_t^2)/E_t + (1 - \nu_s^2)/E_s]^{-1}$ , where  $E_t$  and  $E_s$  are the respective elastic moduli of tip and sample and  $\nu_t$  and  $\nu_s$  are the Poisson ratios.

Typical values of a beam shaped cantilever were used as parameters. In the numerical simulations<sup>1</sup>, three eigenmodes were considered ( $n = 3$ ). For the modal deflection  $\varphi_n$  and deflection angle  $\varphi_n$  the well known eigenmodes of a beam with uniform mass density  $m$  were used [18]. The tip and laser spot were assumed to be collocated at the end of the cantilever beam,  $\xi_{\text{tip}} = \xi_{\text{sens}} = 1$ . The damping was set to  $\gamma_i = 0.0025$  for all modes. Further parameters were:  $k = 10 \text{ N m}^{-1}$ ,  $R = 15 \text{ nm}$ ,  $E_t = 129 \text{ GPa}$ ,  $\nu_t = 0.28$ ,  $E_s = 70 \text{ GPa}$ ,  $\nu_s = 0.3$ ,  $a_0 = 0.166 \text{ nm}$ , and  $H = 6.4 \times 10^{-20} \text{ J}$ . The driving frequency was  $\omega = 1.0$  and the amplitude of the driving force was  $F_{\text{dr}} = 0.97 \text{ nN}$ , resulting in a free amplitude of  $A_0 = 20 \text{ nm}$ .

<sup>1</sup> The simulation was implemented in MATLAB RELEASE 13 using SIMULINK (The Mathworks Inc., Natick, MA, USA).

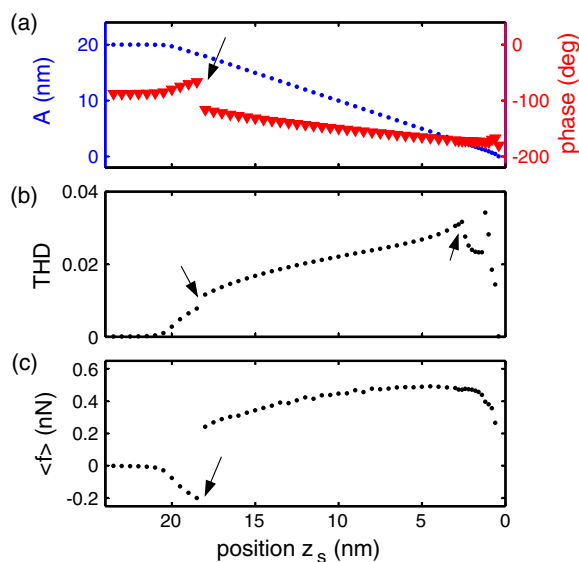


**Figure 2.** (a) Amplitude and phase of the first harmonic. The transition from the low amplitude state into the high amplitude state can be identified by the phase jump (arrow). (b) Total harmonic distortion of the position output. The transition between both states is accompanied by a step in the THD (left-hand arrow). At a small gap  $z_s$ , subharmonics are generated, which leads to a reduction of the THD (right-hand arrow). (c) Average force. The transition from net repulsive to net attractive forces is evident (arrow).

### 3. Results and discussion

To simulate a dynamic AFM spectroscopy experiment, the sample position  $z_s$  was reduced step-wise starting from  $z_s = 24$  nm. In order to obtain data of the equilibrated system, the approach ramp was halted and the system allowed to equilibrate for more than 1000 cycles before the data was extracted for Fourier transform (FFT) analysis. For  $z_s > 3$  nm data was extracted every 0.5 nm; for smaller  $z_s$  this distance was decreased to 0.2 nm to capture the complicated dynamics at small distances. Figure 2 shows the evolution of characteristic values with varying tip-sample gap. The amplitude, phase and average force exhibit the well known features of the SDOF approximation that are due to the transition from the low amplitude state to the high amplitude state [1]. For a further investigation, the anharmonic contributions in the system output (1) were calculated. The harmonic distortion is defined by  $\text{THD} = (\sum_{n=2}^{\infty} |c_n|^2)^{-1/2} / (\sum_{n=1}^{\infty} |c_n|^2)^{-1/2}$ , where  $|c_n|$  is the FFT amplitude of the  $n$ th harmonic. It gives the fraction of power that is contained in the higher harmonics as compared to the total power. Far away from the sample, the oscillation amplitude of the fundamental was  $2|c_1| = 20$  nm and the phase was at  $-90^\circ$ . There was only a very small average attractive force and a very small total harmonic distortion. Approaching  $z_s = 20$  nm the system was in the net attractive (low amplitude) regime as can be seen by the net negative interaction force. With increasing strength of the attractive interaction, the THD of the output signal also increased. Between  $z_s = 18.5$  and 18 nm the system transitioned to the high amplitude state (as shown by the arrows). This transition prevails in the phase as well as in the average interaction force. It is also visible in the THD which increases by 50%. Approaching further, the dynamics

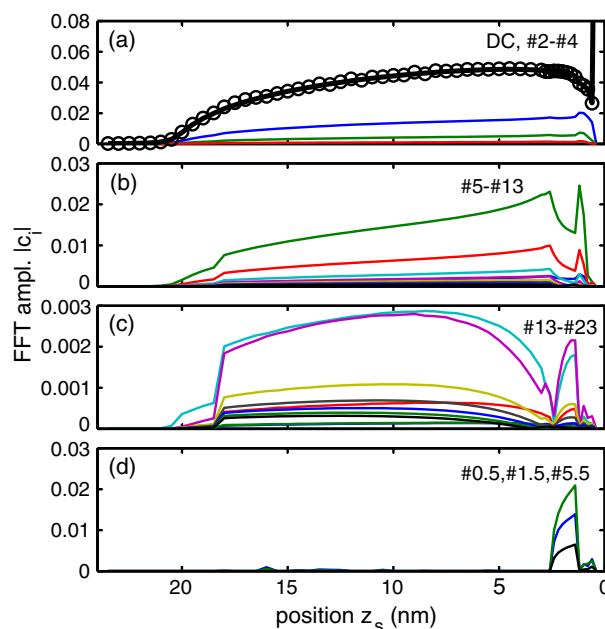


**Figure 3.** (a)–(c) Harmonics as obtained in the position output. They are grouped together according to the eigenmode that contributes most to the respective signal. The dc contribution perfectly coincides with the average tip-sample interaction force (circles). (d) Subharmonics are generated at a small separation between cantilever and sample.

of the system changed at  $z_s = 2.8$  nm. The THD decreased significantly and recovered at  $z_s = 1$  nm before it dropped to zero. This behaviour can be explained by the generation of subharmonics where spectral power is transferred into the subharmonics or by non-periodic dynamics where the power is distributed over the entire spectrum.

In figure 3 the evolution of the harmonics and the subharmonics of the period-2 solution are displayed. The harmonics are grouped according to the eigenmode that contributes most to the respective signal. In figure 3(a) the dc value  $|c_0|$ , also known as the ‘tapping-mode deflection’, is shown together with the amplitudes  $|c_1|$  to  $|c_4|$  that are grouped around the fundamental frequency. The static deflection due to the absolute value of the average force  $\Delta z = | \langle f_{\text{avg}} \rangle | / k$  is superimposed on the plot (circles). It agrees perfectly with the dc value. Thus, the dc value, that can easily be measured in a standard atomic force microscope by low-pass filtering of the signal, can be used as a measure for the average tip-sample force. The group below shows the amplitudes  $|c_5|$  to  $|c_{13}|$  around the second eigenmode. The amplitudes of these harmonics drop with the onset of period doubling. They recover before the amplitudes drop to zero. Together with the harmonics  $|c_1|$  to  $|c_4|$ , the harmonics  $|c_5|$  to  $|c_{13}|$  dominate in the THD. The harmonics grouped around the third mode exhibit a significant jump in the transition from the low amplitude to the high amplitude solution. The subharmonics appear at  $z_s < 2.4$  nm. In figure 3(d) the subharmonics  $\omega/2$ ,  $3/2\omega$ , and  $11/2\omega$  are shown.

For further investigation of the dynamics it is instructive to analyse the spectra at different  $z_s$ . Selected spectra are displayed in figure 4. Far away from the sample surface at  $z_s = 23$  nm there was only a weak anharmonic contribution.

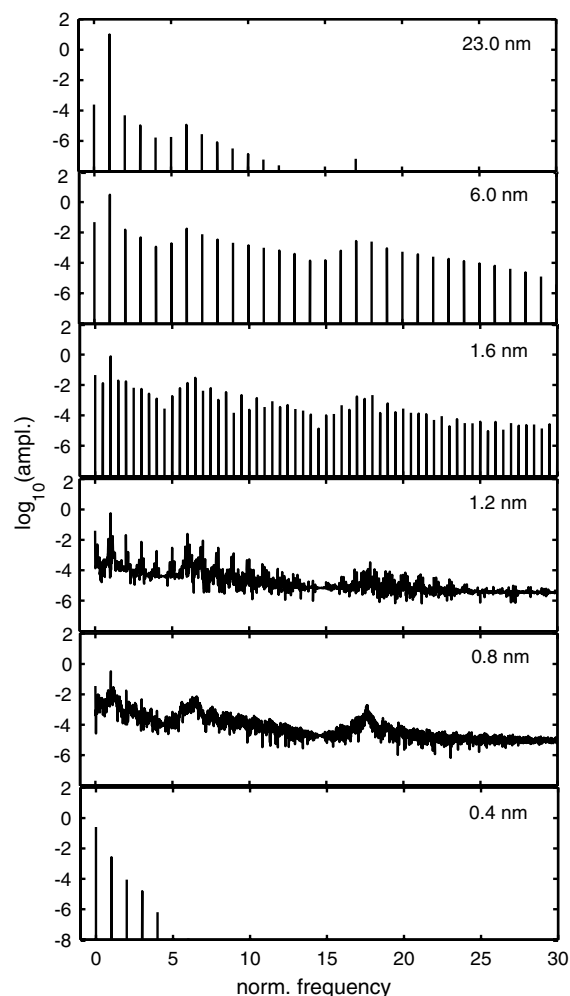


**Figure 4.** Fast Fourier transform of the position output at different tip-sample gaps  $z_s$  as indicated.

Closer to the surface, an entire spectrum of higher harmonics prevailed (see, for example,  $z_s = 6$  nm). At smaller

separations a more complicated dynamics could be observed. At  $z_s = 1.6$  nm the subharmonics were clearly visible, indicating period doubling. At  $z_s = 1.2$  nm the energy was distributed over the entire spectrum although the harmonics are pronounced. This explains the peak in the THD at  $z_s = 1.2$  nm. Approaching further ( $z_s = 0.8$  nm), the energy was distributed over the spectrum and the transfer function of the dynamic system became visible. Finally, at  $z_s = 0.4$  nm the tip snapped on to the surface and was not released any more. The tip was then in contact, which corresponds to the force modulation mode of operation. In the light lever output (2) a signal around the 4th harmonic appeared, which is due to the contact resonance of the system (data not shown). This resonance of the surface coupled cantilever could not be observed in the position output because the position readout was collocated with the tip.

Figure 5 shows the time course of both system outputs and the tip-sample forces. At a tip-sample gap of  $z_s = 4$  nm a strong distortion was visible in both outputs. With a smaller gap at  $z_s = 1.6$  nm, period doubling became evident. This can be seen in the alternating pattern of the signals. Experimentally, a similar signature of period doubling was observed earlier (figure 5(a) in [15]). At smaller gaps, the simulated motion became non-periodic (figure 5(c)). This led to variations of the peak forces of the tip impact on to the specimen. Additionally, multiple impacts could occur.

The simulation results show that the dynamics of the MDOF system is similar to the dynamics as calculated with the widely used SDOF approximation, for large tip-sample gaps. However, at small set-points, the higher eigenmodes of the cantilever contribute to the signal formation as well as to the dynamics of the system. Thus, in order to capture the dynamics at the transition from imaging to nanomanipulation, a higher order MDOF model has to be used in numerical calculations.

This also has consequences for the design of controllers such as  $Q$ -control [19] or chaos control [8] if their use is extended to the small set-point regime. Both controllers require knowledge of  $x_1$  or  $\dot{x}_1$ . However, in most AFM

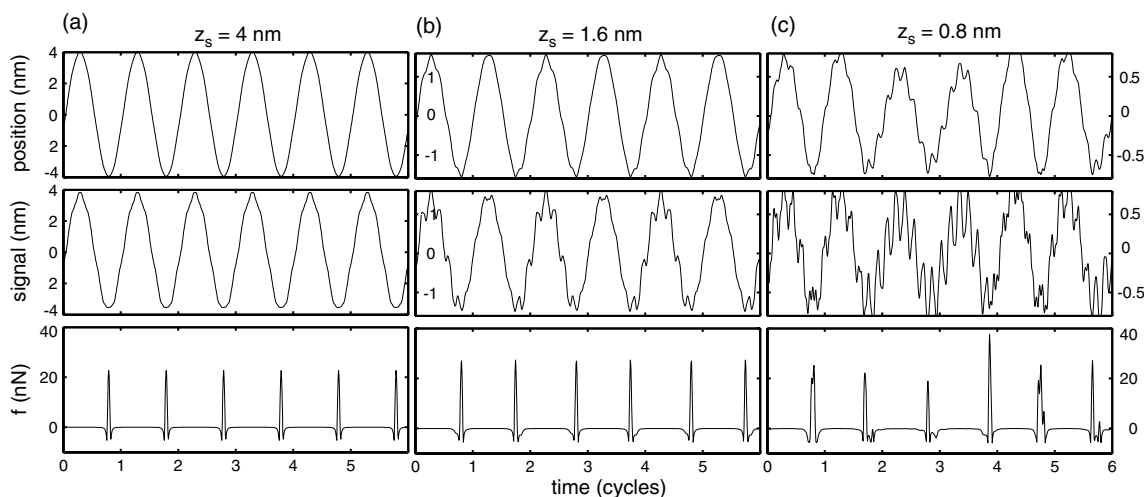


**Figure 5.** Time course of the position (top) and light lever output (middle), together with the tip-sample force (below). (a) The harmonic distortion is evident in the light lever output signal. (b) Period doubling. (c) Non-periodic motion. (An animation shows the output data for the entire approach.)

 A gif movie of this figure is available from [stacks.iop.org/Nano/15/347](https://stacks.iop.org/Nano/15/347)

systems the cantilever deflection angle or the tip displacement is observed using an optical lever or an interferometer, respectively. As shown previously, these measurable quantities are linear combinations of the system states whereas the states themselves are not observable. Thus, in situations where the signals of the higher eigenmodes are not negligible, the observable quantities  $y_1$  or  $y_2$  provide only poor estimates for the system state  $x_1$ . This is also true for the state  $\dot{x}_1$  which is usually determined by applying a  $-90^\circ$  phase shift to the signals  $y_1$  or  $y_2$  with respect to the driving frequency. Thus, appropriate filtering or an observer are required in order to obtain a good estimate of the system states for feedback under these conditions.

#### 4. Conclusions

In conclusion, dynamic AFM was simulated numerically by means of a multiple-degree-of-freedom approach where the cantilever is treated as a linear and time invariant system and the mechanical interaction between tip and sample as a nonlinear output feedback. For the amplitude and phase of the first harmonic the MDOF solution provides similar results to the SDOF solutions. In addition, valuable information about the oscillatory state in dynamic AFM can be obtained by investigation of the spectrum of the system response. The dc part contains the average tip-sample interaction force. Higher harmonics are generated by the nonlinear tip-sample interaction. They are enhanced by the higher eigenmodes. In close proximity to the sample, the higher eigenmodes significantly contribute to the dynamics. This illustrates that MDOF models have to be used to investigate and control the tip-sample forces for small tip-sample gaps.

#### Acknowledgment

This work was supported by the Federal Ministry of Education and Research (BMBF) under Grant 03N8706.

#### References

- [1] García R and Pérez R 2002 *Surf. Sci. Rep.* **47** 197
- [2] Stark R W, Schitter G and Stemmer A 2004 *Phys. Rev. B* in press
- [3] Hunt J and Sarid D 1998 *Appl. Phys. Lett.* **72** 2969
- [4] Basso M, Giarré L, Dahleh M and Mezić I 2000 *J. Dyn. Syst. Meas. Control* **122** 240
- [5] Rützel S, Lee S I and Raman A 2003 *Proc. R. Soc. A* **459** 1925
- [6] Salapaka M V, Chen D J and Cleveland J P 2000 *Phys. Rev. B* **61** 1106
- [7] Ashhab M, Salapaka M, Dahleh M and Mezić I 1999 *Automatica* **35** 1663
- [8] Ashhab M, Salapaka M, Dahleh M and Mezić I 1999 *Nonlinear Dyn.* **20** 197
- [9] Sasaki N, Tsukada M, Tamura M, Tamura R, Abe K and Sato N 1998 *Appl. Phys. A* **66** S287
- [10] Burnham N A, Kulik A J, Gremaud G and Briggs G A D 1995 *Phys. Rev. Lett.* **74** 5092
- [11] Stark R W and Heckl W M 2000 *Surf. Sci.* **457** 219
- [12] Sahin O and Atalar A 2001 *Appl. Phys. Lett.* **79** 4455
- [13] Rodríguez T R and García R 2002 *Appl. Phys. Lett.* **80** 1646
- [14] Balantekin A and Atalar A 2003 *Phys. Rev. B* **67** 193404
- [15] Stark M, Stark R W, Heckl W M and Guckenberger R 2002 *Proc. Natl Acad. Sci. USA* **99** 8473
- [16] Stark M, Stark R W, Heckl W M and Guckenberger R 2000 *Appl. Phys. Lett.* **77** 3293
- [17] Derjaguin B V, Muller V M and Toporov Yu P 1975 *J. Colloid Interface Sci.* **53** 314
- [18] Clough R and Penzien J 1993 *Dynamics of Structures* 2nd edn (Singapore: McGraw-Hill)
- [19] Anczykowski B, Cleveland J P, Krueger D, Elings V and Fuchs H 1998 *Appl. Phys. A* **66** S885